Physics Letters A 382 (2018) 1379–1382

Contents lists available at ScienceDirect

Physics Letters A

www.elsevier.com/locate/pla

Concentric layered Hermite scatterers

Jeffrey P. Astheimer [a], Kevin J. Parker [b,*]

[a] HABICO, Inc., Rochester, NY, USA
[b] Department of Electrical and Computer Engineering, University of Rochester, Hopeman Building 203, Box 270126, Rochester, NY 14627, USA

ARTICLE INFO

Article history:
Received 23 January 2018
Received in revised form 6 March 2018
Accepted 24 March 2018
Available online 28 March 2018
Communicated by M.G.A. Paris

Keywords:
Rayleigh scattering
Electromagnetics
Optics
Acoustics
Hermite polynomials
Contrast agents

ABSTRACT

The long wavelength limit of scattering from spheres has a rich history in optics, electromagnetics, and acoustics. Recently it was shown that a common integral kernel pertains to formulations of weak spherical scatterers in both acoustics and electromagnetic regimes. Furthermore, the relationship between backscattered amplitude and wavenumber k was shown to follow power laws higher than the Rayleigh scattering k^2 power law, when the inhomogeneity had a material composition that conformed to a Gaussian weighted Hermite polynomial. Although this class of scatterers, called Hermite scatterers, are plausible, it may be simpler to manufacture scatterers with a core surrounded by one or more layers. In this case the inhomogeneous material property conforms to a piecewise continuous constant function. We demonstrate that the necessary and sufficient conditions for supra-Rayleigh scattering power laws in this case can be stated simply by considering moments of the inhomogeneous function and its spatial transform. This development opens an additional path for construction of, and use of scatterers with unique power law behavior.

1. Introduction

The phenomenon of Rayleigh scattering in optics and acoustics has provided many familiar examples of long wavelength scattered amplitude proportional to k^2 where k is the wavenumber. Recently, Parker [14] demonstrated that a new class of weak spherically symmetric scatterers, designated as Hermite scatterers, could produce long wavelength backscatter amplitude proportional to k^4, k^6, and higher even powers of wavelength. The material properties of the inhomogeneity are required to conform to a modified Gaussian weighted Hermite polynomial function of odd order, producing the pure power law limit for scattering. Parker also demonstrated that a common integral kernel exists across acoustic and electromagnetic scattering theories in the Born approximation, and so the formulation of Hermite scatterers is valid for optical and acoustical material properties. With advances in nanotechnology manufacturing techniques, it is possible to construct spherical nanoparticles that have variable material properties as a function of radius, and so the use of unique orders of Hermite scatterers as contrast agents or dye indicators is plausible.

However, one disadvantage of formulating Hermite Scatterers is that the material properties must conform to a smooth, continuously varying spatial function, at least to a radius that extends three or four standard deviations of the Gaussian weighting function. In some cases it may be easier to manufacture a spherical core of one material with discrete outer layers of different materials, each one possessing a unique property: index of refraction or bulk compressibility. In this case the spherical inhomogeneity would have a piecewise continuous function from radius $r = 0$ to some maximum value representing the outer diameter of the outermost layer. This paper considers the mathematics of the layered scatterer and derives some simple requirements involving the moments of the scattering integral, such that supra-Rayleigh long wavelength power laws can be achieved.

2. Theory

To derive the equation for backscattered pressure P_{bs} from an acoustic inhomogeneity, we follow the classical approach described in Chapter 8 of Morse and Ingard [11]. Under the Born approximation (weak scatterers) with an incident plane wave of amplitude A and frequency ω traveling in the x-direction; $k = \omega/c$ is the wavenumber and c is the speed of sound:

$$P_{bs}(k, x) \cong A\left(\frac{\mathbf{e}^{ikx}}{x}\right)\phi_s(k), \tag{1}$$

where

* Corresponding author.
E-mail address: kevin.parker@rochester.edu (K.J. Parker).

https://doi.org/10.1016/j.physleta.2018.03.041
0375-9601/

$$\phi_s(k) = \left(\frac{k^2}{4\pi}\right) \iiint \kappa(r)\, \mathbf{e}^{i2\hat{\mathbf{k}}\bullet\hat{\mathbf{r}}} dVol, \tag{2}$$

and where $\kappa(r)$ is the (small) fractional change in compressibility within the scatterer, assumed to vary only in the radial dimension, the $2\hat{k}$ term in the complex exponential comes from the 180° direction of backscatter, and the integration is over the scattering volume. In summary, the backscatter formula can be written as:

$$P_{bs}(k,x) = A\left(\frac{\mathbf{e}^{jkx}}{x}\right)\left(\frac{k^2}{4\pi}\right) \iiint \kappa(r)\, \mathbf{e}^{j2\hat{\mathbf{k}}\cdot\hat{\mathbf{r}}} dVol. \tag{3}$$

Note that a similar integral kernel applies to scattering from weak electromagnetic inhomogeneities [14], as well.

Now let

$$\mathrm{K}(k) = \iiint \kappa(r)\, \mathbf{e}^{j2\hat{\mathbf{k}}\cdot\hat{\mathbf{r}}} dVol \tag{4}$$

denote the (radial) inverse three dimensional transform of $\kappa(r)$. The long-wavelength behavior of $P_{bs}(k,x)$ is determined by the long-wavelength behavior of $\mathrm{K}(k)$ which, in turn, is determined by the Taylor expansion

$$\mathrm{K}(k) = \mathrm{K}(0) + \mathrm{K}'(0)\,k + \frac{\mathrm{K}''(0)\,k^2}{2} + \cdots \tag{5}$$

However, since $\mathrm{K}(k) = \mathrm{K}\left(\left\|\hat{\boldsymbol{k}}\right\|\right)$ has radial symmetry the odd terms in the above expansion are 0, and therefore:

$$\mathrm{K}(k) = \mathrm{K}(0) + \frac{\mathrm{K}''(0)\,k^2}{2} + \frac{\mathrm{K}^{(iv)}(0)\,k^4}{4!} \cdots \tag{6}$$

This expansion indicates that

$$\begin{aligned} &P_{bs}(k,x) \text{ will have } k^2 \text{ long-wavelength} \\ &\quad\text{(classical Rayleigh) scattering if } \mathrm{K}(0) \neq 0; \\ &P_{bs}(k,x) \text{ will have } k^4 \text{ long-wavelength} \\ &\quad\text{behavior if } \mathrm{K}(0) = 0,\ \mathrm{K}''(0) \neq 0; \\ &P_{bs}(k,x) \text{ will have } k^6 \text{ long-wavelength} \\ &\quad\text{behavior if } \mathrm{K}(0) = 0,\ \mathrm{K}''(0) = 0,\ \mathrm{K}^{(iv)}(0) \neq 0, \text{ etc.} \end{aligned} \tag{7}$$

Next note that even derivatives of K at zero may be expressed in terms of multiple Laplacian operators applied to $\mathrm{K}\left(\left\|\hat{\boldsymbol{k}}\right\|\right)$. (See a proof of this assertion in the appendix.) In the simplest case,

$$\mathrm{K}''(0) = \frac{1}{3}\left[\Delta \mathrm{K}\left(\left\|\hat{\boldsymbol{k}}\right\|\right)\right]_{\hat{\boldsymbol{k}}=0}, \tag{8}$$

and, hence, $\mathrm{K}''(0)$ will vanish if and only if

$$0 = \left[\iiint r^2 \kappa(r)\, \mathbf{e}^{j2\hat{\mathbf{k}}\cdot\hat{\mathbf{r}}} dVol\right]_{\hat{\boldsymbol{k}}=0} = \int r^4 \kappa(r)\, dr. \tag{9}$$

In other words, the long-wavelength behavior of the backscattered response is determined by how many even moments (excluding the 0-th moment) of $\kappa(r)$ vanish. The modified Hermite functions described in [14] satisfy the appropriate moment conditions provided that the limits of integration extend over all space. In that case we let

$$\kappa_m(r) = \frac{\mathbf{G}H_m(r/R)}{r} \tag{10}$$

designate a "Hermite scatterer," where $m \in$ odd integer ≥ 1; R is a reference radius or scale factor, $\mathbf{G}H_m(r/R) = \mathbf{e}^{-(r/R)^2} H_m(r/R)$, and H_m is the mth order Hermite polynomial formed through the mth differentiation of a Gaussian function [1,17]. The odd orders are chosen as they approach zero as $r \to 0$, however the quotient $\mathbf{G}H_m(r/R)/r$ reaches a finite maximum at $r = 0$ by L'Hopital's rule.

In this case, substituting eqn (10) into eqn (4) and converting to spherical coordinates results in

$$\begin{aligned} \mathrm{K}(k) &= \int_{r=0}^{\infty}\int_{\theta=0}^{\pi}\int_{\phi=0}^{2\pi} r \cdot \mathbf{G}H_m\left(\frac{r}{R}\right) \cdot \mathbf{e}^{i2kr\cos\theta} \sin\theta\, dr d\theta d\phi \\ &= \frac{2\pi}{k}\int_{r=0}^{\infty} \mathbf{G}H_m\left(\frac{r}{R}\right) \cdot \sin 2kr dr. \end{aligned} \tag{11}$$

In the form of eqn (2):

$$\phi_s(k) = \left(\frac{k^2}{4\pi}\right)\mathrm{K}(k) = -\sqrt{\pi}2^{(m-2)} \cdot \mathbf{e}^{-(kR)^2} \cdot \left(-k^2R^2\right)^{\frac{m+1}{2}}. \tag{12}$$

For example, if $\kappa_m(r/R) = \kappa_7(r/R) = \mathbf{G}H_7(r/R)/r$, then $\phi_s(k)|_{m=7} = -\sqrt{\pi}32\mathbf{e}^{-(kR)^2}(kR)^8$. Thus, the leading non-zero power law expansion in k for the continuous Hermite scatterer of odd order m is always of order $m+1$.

However, piece-wise continuous functions of finite extent with vanishing moments are also easily generated. For example, a scatterer consisting of a homogeneous sphere encased in a spherical shell of a different material is specified by four parameters (the inner and outer radii and the κ values of the inner and outer materials). These parameters can be selected so that the second and fourth moments of $\kappa(r)$ vanish.

For example, consider a two material sphere of inner core κ_1 for $0 < r < r_1$, and κ_2 for $r_1 < r < r_2$. Setting $K(0)$ to zero requires:

$$\begin{aligned} 0 = K(0) &= \int_0^{r_1} r^2\kappa_1 dr + \int_{r_1}^{r_2} r^2\kappa_2 dr, \text{ or} \\ \kappa_2 &= -\left(\frac{r_1^3}{r_2^3 - r_1^3}\right)\kappa_1. \end{aligned} \tag{13}$$

This condition is necessary for supra-Rayleigh scattering. In practical terms, if $\kappa_1 = 1$, $r_1 = 1$, and $r_2 = 2$ units, then $\kappa_2 = -1/7$. Fig. 1 demonstrates a comparison between the continuous Hermite scatterer of order 3 and the concentric core, with an outer layer described in eqn (13).

3. Discussion

Generalizing these requirements to additional layers and higher moments, we note that a homogeneous sphere encased in two spherical shells of different materials provides enough parameters to null the second and fourth moments of $\kappa(r)$ and that the material parameters for the three components can be found for any choice of three increasing radii. To verify this, let the radii $0 < r_1 < r_2 < r_3$ be chosen arbitrarily, let κ_1, κ_2, and κ_3 be the material parameters of the three shells, and let M_{nm} denote the $2n$-th moment ($n = 1, 2$) of a sphere with radius r_m that has material parameter $\kappa = 1$ (hence $M_{nm} = \int_0^{r_m} r^{2n} dVol = 4\pi \int_0^{r_m} r^{2n+2} dr = 4\pi r_m^{2n+3}/(2n+3)$). Then the second and fourth moments M_1, M_2 of the 3-component scatterer are given by:

$$\begin{aligned} M_1 &= M_{11}\kappa_1 + (M_{12} - M_{11})\,\kappa_2 + (M_{13} - M_{12})\,\kappa_3 \\ M_2 &= M_{21}\kappa_1 + (M_{22} - M_{21})\,\kappa_2 + (M_{23} - M_{22})\,\kappa_3. \end{aligned} \tag{14}$$

Setting $M_1 = M_2 = 0$ results in a degenerate system of two equations in the three unknowns κ_1, κ_2, κ_3, which always has non-zero solutions. Omitting the outer shell, though, results in the equations:

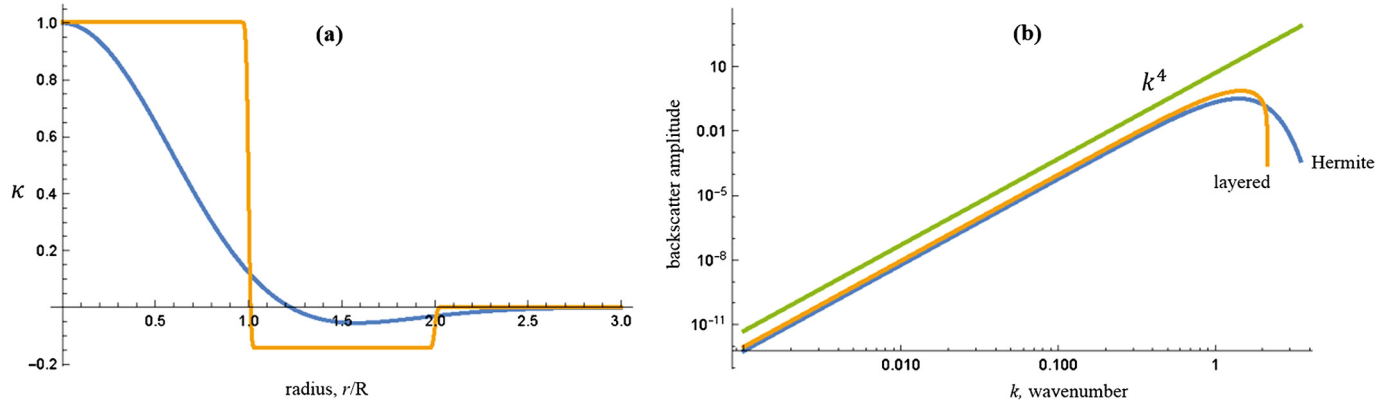

Fig. 1. Comparison of continuous Hermite material properties vs. discrete layers. In (a), the inhomogeneity parameter κ is depicted as related to a third-order Gaussian weighted Hermite function (smooth curve) or else as a piecewise continuous function representing an inner core and an outer layer, with the properties following the necessary requirement of eqn (13). In (b), a log–log plot shows the backscattered amplitude proportional to wavenumber to the fourth power, a supra-Rayleigh dependence. The continuous and the discrete layered scatterers are nearly indistinguishable in backscatter throughout the long wavelength regime.

$$M_1 = M_{11}\kappa_1 + (M_{12} - M_{11})\,\kappa_2$$
$$M_2 = M_{21}\kappa_1 + (M_{22} - M_{21})\,\kappa_2, \tag{15}$$

which only has the solution $\kappa_1 = \kappa_2 = 0$ because the way that M_m are defined insures that eqn (15) is non-degenerate. A straightforward extension of this argument shows that a $(N+1)$-component radial scatterer can be designed to zero the first N even moments.

The role of nanoparticles and core-and-shell formulations is well established in optics and bio-optics [8,10,5]. A range of materials have been employed, including silica [3,24,4,13], gold [9,8], and other compounds [7,6] with core radii often in the 10 nm–200 nm range but shell layers as small as 4 nm have been produced [18].

Core-and-shell formulations are also well utilized in biomedical ultrasound for contrast enhancement [12,16] and sizes are typically below 8 μm in diameter for passage through capillaries. However, many ultrasound contrast agents employ perfluorocarbons [19] for high impedance mismatch with the blood. The associated nonlinear effects and strong scattering would complicate the simple weak scattering (Born approximation) formulation used in the analysis. However, other materials including proteins, lipids, polymers, and gold are also utilized as biocompatible materials [16].

As for size and thickness requirements, let us take $kR_2 = 1$ as the approximate upper limit of supra-Rayleigh scattering, where R_2 is the outer shell radius of the example in eqn (13) and Fig. 1. This places an upper bound on R_2 as $R_2 < \lambda/2\pi$ and for UVA ($\lambda \approx 400$ nm) this limit is 63 nm. For bio-ultrasound at 10 MHz ($\lambda = 0.15$ mm), the requirement would be $R_2 < 24$ μm. In both cases, the size and thickness requirements are well within currently achievable shell dimensions. The next important issue would be achieving the ratio of material properties κ_2/κ_1 prescribed by eqn (13), including the requirement for one material to have a higher index of refraction (or acoustic impedance) than the reference medium, and the other material to have a lower index of refraction (or acoustic impedance). In many biomedical applications, the reference medium is aqueous, and so concentric scatterer materials would be assessed with respect to the material properties of water or saline. For optical scatterers this requires candidate materials above and below the reference index of refraction of 1.33 for water. Lower index of refraction (range 1.05 to 1.3) materials already used in optical tracers include aerogels, perfluorocarbons, and emulsions of gold nanoparticles [8,21,19,23,2]. Higher values (range 1.35 to above 2.0) are achieved with many materials including glycerol, collagens, proteins, oils, organometallic, and silica compounds [22].

For bioacoustics, the compressibility of water (2.2 GPa bulk modulus; the inverse of compressibility) represents a key property of the reference medium. Commonly employed contrast materials with higher compressibility include perfluorocarbons, aerogels, and oils. Lower compressibility materials include some collagens and polymers, along with organometallic compounds [20]. Additionally, in a full treatment of acoustic backscatter, the density of the scatterers also contributes [11]. Some x-ray contrast materials containing iodine have much higher density than water, for example solid iodipamide ethyl ester microparticles have a density of 2.4 g/ml [15,12], whereas many oils and fats have lower densities [20].

4. Conclusion

Supra-Rayleigh scattering may be useful in a variety of applications such as tracers and contrast agents. We now have two approaches to the mathematical requirements of the inhomogeneous material properties (index of refraction in the case of optics, or else compressibility or density in the case of acoustics) so as to produce supra-Rayleigh scattering behavior in the long wavelength regime. In the case where the properties can conform to a continuous function of radius, the modified Gaussian weighted Hermite polynomials of odd orders specify higher power law scattering. In the case where the material properties are constructed from an inner spherical core with one or more layers, the scattering power laws can be prescribed by considering the necessary conditions of zero moments. In practical terms, these require a choice of inhomogeneities that have both positive and negative values (in weak scattering this corresponds to material properties that are slightly higher than and slightly lower than those of the reference medium, respectively) and that can be formulated with a high degree of precision in the material properties and the spatial arrangement of the layers.

Acknowledgements

We are indebted to Professor Robert Waag for his illuminating explanations of scattering, and to HABICO, Inc. for their expertise. This work was supported by the Hajim School of Engineering and Applied Sciences at the University of Rochester.

Appendix

The computations below derive the relationship $\mathrm{K}^{(2n)}(0) = \frac{1}{2n+1}\left[\Delta^n \mathrm{K}\left(\left\|\hat{\boldsymbol{k}}\right\|\right)\right]_{\hat{\boldsymbol{k}}=0}$ between the even derivatives of K at the origin and the even moments of $\kappa(r)$ that was asserted to exist in the discussion above. Note that $\Delta \mathrm{K}\left(\left\|\hat{\boldsymbol{k}}\right\|\right) = \left(\frac{d^2}{dk^2} + \frac{2}{k}\frac{d}{dk}\right)\mathrm{K}(k)$ and

hence $\Delta^n \mathrm{K}\left(\left\|\hat{\boldsymbol{k}}\right\|\right) = \left(\frac{d^2}{dk^2} + \frac{2}{k}\frac{d}{dk}\right)^n \mathrm{K}(k)$. The value of $[\Delta^n \mathrm{K}(\|\hat{\boldsymbol{k}}\|)]_{\hat{\boldsymbol{k}}=0}$ can then be evaluated by expanding the operator $(\frac{d^2}{dk^2} + \frac{2}{k}\frac{d}{dk})^n$, applying the expansion to $\mathrm{K}(k)$, and evaluating the result at $k = 0$. The operator expansion is obtained by means of the recursion formula:

$$\left(\frac{d^2}{dk^2} + \frac{2}{k}\frac{d}{dk}\right)\left(\frac{d^{2n-2}}{dk^{2n-2}} + \frac{2n-2}{k}\frac{d^{2n-3}}{dk^{2n-3}}\right) = \left(\frac{d^{2n}}{dk^{2n}} + \frac{2}{k}\frac{d^{2n-1}}{dk^{2n-1}}\right) \tag{16}$$

that is shown by the expansion:

$$\begin{aligned}
&\left(\frac{d^2}{dk^2} + \frac{2}{k}\frac{d}{dk}\right)\left(\frac{d^{2n-2}}{dk^{2n-2}} + \frac{2n-2}{k}\frac{d^{2n-3}}{dk^{2n-3}}\right)\\
&= \frac{d^{2n}}{dk^{2n}} + \frac{d^2}{dk^2}\left(\frac{2n-2}{k}\frac{d^{2n-3}}{dk^{2n-3}}\right)\\
&\quad + \frac{2}{k}\frac{d^{2n-1}}{dk^{2n-1}} + \frac{2(2n-2)}{k^2}\frac{d^{2n-2}}{dk^{2n-2}} - \frac{4(2n-2)}{k^3}\frac{d^{2n-3}}{dk^{2n-3}}\\
&= \frac{d^{2n}}{dk^{2n}} + \frac{d}{dk}\left(\frac{2n-2}{k}\frac{d^{2n-2}}{dk^{2n-2}} - \frac{2(2n-2)}{k^2}\frac{d^{2n-3}}{dk^{2n-3}}\right)\\
&\quad + \frac{2}{k}\frac{d^{2n-1}}{dk^{2n-1}} + \frac{2(2n-2)}{k^2}\frac{d^{2n-2}}{dk^{2n-2}} - \frac{4(2n-2)}{k^3}\frac{d^{2n-3}}{dk^{2n-3}}\\
&= \frac{d^{2n}}{dk^{2n}} + \left(\frac{2n-2}{k}\frac{d^{2n-1}}{dk^{2n-1}} - \frac{2(2n-2)}{k^2}\frac{d^{2n-2}}{dk^{2n-2}}\right.\\
&\quad \left. + \frac{4(2n-2)}{k^3}\frac{d^{2n-3}}{dk^{2n-3}}\right)\\
&\quad + \frac{2}{k}\frac{d^{2n-1}}{dk^{2n-1}} + \frac{2(2n-2)}{k^2}\frac{d^{2n-2}}{dk^{2n-2}} - \frac{4(2n-2)}{k^3}\frac{d^{2n-3}}{dk^{2n-3}}\\
&= \frac{d^{2n}}{dk^{2n}} + \frac{2n}{k}\frac{d^{2n-1}}{dk^{2n-1}}.
\end{aligned} \tag{17}$$

A simple induction argument then gives:

$$\left(\frac{d^2}{dk^2} + \frac{2}{k}\frac{d}{dk}\right)^n = \left(\frac{d^{2n}}{dk^{2n}} + \frac{2n}{k}\frac{d^{2n-1}}{dk^{2n-1}}\right). \tag{18}$$

This result gives:

$$\begin{aligned}
\Delta^n \mathrm{K}\left(\left\|\hat{\boldsymbol{k}}\right\|\right) &= \left(\frac{d^2}{dk^2} + \frac{2}{k}\frac{d}{dk}\right)^n \mathrm{K}(k)\\
&= \left(\frac{d^{2n}}{dk^{2n}} + \frac{2n}{k}\frac{d^{2n-1}}{dk^{2n-1}}\right)\mathrm{K}(k)\\
&= \mathrm{K}^{(2n)}(k) + 2n\frac{\mathrm{K}^{(2n-1)}(k)}{k}.
\end{aligned} \tag{19}$$

Finally, note that L'Hopital's rule can be used to evaluate the second term on the right at $k = 0$ (since both the numerator and denominator vanish at $k = 0$), yielding the final result

$$\left[\Delta^n \mathrm{K}\left(\left\|\hat{\boldsymbol{k}}\right\|\right)\right]_{\hat{\boldsymbol{k}}=0} = (2n+1)\,\mathrm{K}^{(2n)}(0). \tag{20}$$

References

[1] M. Abramowitz, I.A. Stegun, Handbook of Mathematical Functions with Formulas, Graphs, and Mathematical Tables, U.S. Govt. Print. Off., Washington, 1964.
[2] H. Chen, X. Kou, Z. Yang, W. Ni, J. Wang, Shape- and size-dependent refractive index sensitivity of gold nanoparticles, Langmuir 24 (2008) 5233–5237.
[3] C. Graf, W. Schärtl, K. Fischer, N. Hugenberg, M. Schmidt, Dye-labeled poly(organosiloxane) microgels with core–shell architecture, Langmuir 15 (1999) 6170–6180.
[4] C. Graf, D.L.J. Vossen, A. Imhof, A. van Blaaderen, A general method to coat colloidal particles with silica, Langmuir 19 (2003) 6693–6700.
[5] M.A. Hahn, A.K. Singh, P. Sharma, S.C. Brown, B.M. Moudgil, Nanoparticles as contrast agents for in-vivo bioimaging: current status and future perspectives, Anal. Bioanal. Chem. 399 (2011) 3–27.
[6] C.D. Jones, L.A. Lyon, Dependence of shell thickness on core compression in acrylic acid modified poly(N-isopropylacrylamide) core/shell microgels, Langmuir 19 (2003) 4544–4547.
[7] G.H. Koenderink, S. Sacanna, C. Pathmamanoharan, M. Rașa, A.P. Philipse, Preparation and properties of optically transparent aqueous dispersions of monodisperse fluorinated colloids, Langmuir 17 (2001) 6086–6093.
[8] T.M. Lee, A.L. Oldenburg, S. Sitafalwalla, D.L. Marks, W. Luo, F.J. Toublan, K.S. Suslick, S.A. Boppart, Engineered microsphere contrast agents for optical coherence tomography, Opt. Lett. 28 (2003) 1546–1548.
[9] L.M. Liz-Marzán, M. Giersig, P. Mulvaney, Synthesis of nanosized gold-silica core-shell particles, Langmuir 12 (1996) 4329–4335.
[10] C. Loo, A. Lin, L. Hirsch, M.H. Lee, J. Barton, N. Halas, J. West, R. Drezek, Nanoshell-enabled photonics-based imaging and therapy of cancer, Technol. Cancer Res. Treat. 3 (2004) 33–40.
[11] P.M.C. Morse, K.U. Ingard, Theoretical Acoustics, Princeton University Press, Princeton, 1968.
[12] J. Ophir, K.J. Parker, Contrast agents in diagnostic ultrasound, Ultrasound Med. Biol. 15 (1989) 319–333.
[13] H. Ow, D.R. Larson, M. Srivastava, B.A. Baird, W.W. Webb, U. Wiesner, Bright and stable core-shell fluorescent silica nanoparticles, Nano Lett. 5 (2005) 113–117.
[14] K.J. Parker, Hermite scatterers in an ultraviolet sky, Phys. Lett. A 381 (2017) 3845–3848.
[15] K.J. Parker, T.A. Tuthill, R.M. Lerner, M.R. Violante, A particulate contrast agent with potential for ultrasound imaging of liver, Ultrasound Med. Biol. 13 (1987) 555–566.
[16] R.H. Perera, C. Hernandez, H. Zhou, P. Kota, A. Burke, A.A. Exner, Ultrasound imaging beyond the vasculature with new generation contrast agents, Wiley Interdiscip. Rev. Nanomed. Nanobiotechnol. 7 (2015) 593–608.
[17] A.D. Poularikas, Transforms and Applications Handbook, CRC Press, Boca Raton, Fla, 2010.
[18] E. Prodan, C. Radloff, N.J. Halas, P. Nordlander, A hybridization model for the plasmon response of complex nanostructures, Science 302 (2003) 419–422.
[19] E.G. Schutt, D.H. Klein, R.M. Mattrey, J.G. Riess, Injectable microbubbles as contrast agents for diagnostic ultrasound imaging: the Key role of perfluorochemicals, Angew. Chem., Int. Ed. Engl. 42 (2003) 3218–3235.
[20] A.R. Selfridge, Approximate material properties in isotropic materials, IEEE Trans. Sonics Ultrason. 32 (1985) 381–394.
[21] B.E. Smart, Fluorine substituent effects (on bioactivity), J. Fluorine Chem. 109 (2001) 3–11.
[22] J.G. Speight, N.A. Lange, Lange's Handbook of Chemistry, McGraw–Hill, New York, 2005.
[23] M. Tabata, I. Adachi, T. Fukushima, H. Kawai, H. Kishimoto, A. Kuratani, H. Nakayama, S. Nishida, T. Noguchi, K. Okudaira, Y. Tajima, H. Yano, H. Yokogawa, H. Yoshida, Development of silica aerogel with any density, in: IEEE Nuclear Science Symposium Conference Record, 2005, 2005, pp. 816–818.
[24] K.P. Velikov, A. van Blaaderen, Synthesis and characterization of monodisperse core-shell colloidal spheres of zinc sulfide and silica, Langmuir 17 (2001) 4779–4786.